ELSEVIER

Thermochimica Acta 278 (1996) 9–18

thermochimica
acta

Characterisation of amorphous materials by modulated differential scanning calorimetry

Corrado Tomasi[a,*], Piercarlo Mustarelli[a], Nick A. Hawkins[b],
Vivienne Hill[b]

[a] *C.S.T.E.-C.N.R. and Dipartimento di Chimica Fisica Università di Pavia, Viale Taramelli 16, 27100 Pavia, Italy*
[b] *TA Instruments, Europe House, Bilton Centre, Leatherhead, Surrey, UK*

Received 7 July 1995; accepted 7 November 1995

Abstract

This paper investigates the potential of the Modulated Differential Scanning Calorimetry (MDSC^{TM}) technique in the thermal characterisation of various amorphous materials. Inorganic glasses, composites and glass–polymer mixed materials have been investigated in order to separate the glass transition from irreversible phenomena, such as cold crystallisation or residual cure. This new technique requires some additional experimental parameters to be set, whose role in affecting thermal signals is also briefly discussed.

Keywords: Composites; Glasses; Modulated DSC; Thermal analysis; Thermodynamics

1. Introduction

Amorphous materials, such as organic and inorganic polymers, glasses and composites, are currently very promising subjects in materials science because of their technological applications as functional as well as structural components. Because of their lack of structural periodicity, amorphous materials cannot be easily studied by means of traditional diffractometric techniques, whereas most common spectroscopic techniques generally do not offer easy-to-interpret data. In addition, polymers and glasses are thermodynamically metastable, and their structural relaxations must be taken into account when they are investigated for technological applications. In this respect, thermal analysis may play a fundamental role.

---

[*] Corresponding author.

SSDI 0040-6031(95)02786-6

Differential scanning calorimetry (DSC) is by far the most common dynamic technique used in calorimetry and thermal analysis. In this approach, the heat flow rate associated with a thermal event can be measured as a function of time and temperature, allowing us to obtain quantitative information about heat capacities or phase transitions.

DSC measurements are generally affected by a number of factors which, in part, are related to the sample features (geometry, particle size, mass, thermal conductivity, sample-pan contact surface) and, in part, are dependent on the experimental conditions (scanning rate, atmosphere). Some of these effects, namely particle size and the mass of the sample, heating rate and atmosphere have been recently investigated both experimentally and theoretically [1–3]. In addition, the intrinsic dynamic character of DSC requires scientists to evaluate carefully how these experimental parameters may influence the measurements [4–6]. Computer simulations of a heat-flux DSC experiment have been carried out using a model based on the equivalence between thermal and electrical resistances and capacities [7].

An important and recent improvement in standard DSC which has been developed by TA Instruments is modulated DSC (MDSC™) [8]. With MDSC™, a sinusoidal wave is superimposed onto the conventional linear temperature ramp, resulting in an oscillating profile of specific frequency and amplitude. Being an extension of standard DSC, MDSC™ not only provides the same information about the heat associated with various phenomena, but also discriminates between reversing and non-reversing events in the time period of the experimental parameters (see next section).

The aim of this work is to highlight the advantages and limitations of MDSC™ when studying true irreversible phenomena, such as cold crystallisations in glasses and polymers or residual curing in resins, as well as other thermal features related to the choice of experimental parameters, e.g. enthalpic relaxation at the glass transition, which may be termed as pseudo-irreversible phenomena. For this reason, a number of samples of various amorphous materials (glasses and composites) have been examined by means of this technique over a wide range of temperatures.

2. Theoretical background

The most common differential scanning calorimeters available commercially are the power compensating DSC and the heat flux DSC.

The former is based on the principle that, during a run, both sample and reference must always be kept at the same temperature. This can be realised by means of two different heaters that separately provide the required amount of heat per unit of time. The differential power is thus recorded as a function of temperature or time.

The heat flux DSC employs a single heating block and is somewhat different in principle. In this case, the differential heat flow rate is related to the temperature difference between sample and reference. The equivalence of the heat flow paths between the sample and reference is realised by optimising the design of the heat transfer medium and thermocouple positions [9].

Such an approach allows the measurement of heats of transition and heat capacities with good accuracy (of the order of a few percent) and reproducibility. In addition, if compared with adiabatic calorimeters, both heat flux DSC and power compensating DSC can be used for more rapid enthalpy determinations over a broader range of temperature (from −170°C up to 725°C) even though their precision is lower by one order of magnitude.

MDSC$^{\mathrm{TM}}$ is a recent extension of the standard heat-flux DSC, having the same cell arrangement and more sophisticated temperature profile capabilities. In this case, a sinusoidal wave is superimposed to the normal linear temperature ramp

$$T(t) = T_0 + \beta t + A_{\mathrm{T}} \sin(\omega t) \tag{1}$$

where $T(t)$ is the program temperature, T_0 is the starting temperature, β is the underlying average heating rate, and $\omega = 2\pi v$ is the modulation angular frequency.

Generally speaking, in a conventional heat flux DSC the difference between sample and reference heat flows can be expressed by the thermal equivalent Ohm's law

$$\mathrm{d}Q = \frac{\mathrm{d}T}{R} \tag{2}$$

where $\mathrm{d}T$ is the temperature difference measured between sample and reference, and R is the thermal resistance of the cell. In the case of MDSC, heat flow could be represented by the equation

$$\frac{\mathrm{d}Q}{\mathrm{d}T} = \frac{\mathrm{d}T}{\mathrm{d}t} C_{\mathrm{p}} + f(t, T) + f'(t, T) \tag{3}$$

where $\mathrm{d}Q/\mathrm{d}t$ is the heat flow rate out of the sample, $\mathrm{d}T/\mathrm{d}t$ is the heating rate, C_{p} is the sample heat capacity, $f'(t, T)$ is the thermodynamic irreversible heat flow rate component, and $f(t, T)$ is the kinetically-limited heat flow rate. In detail, function f' represents the contribution to the total heat flow rate given by true irreversible phenomena, which imply a transformation from metastable to thermodynamically stable states. In contrast, f represents the contribution to the total heat flow rate given by those reversible phenomena taking place with a kinetics that is slow when compared with the experimental timescale.

As evidenced by Eq. (1), an MDSC analysis requires the setting of two other parameters in addition to the heating rate, namely the frequency and the amplitude of the sine-wave temperature modulation. By this technique, not only total heat flow rate but also heat flow amplitude, which is proportional to heat capacity, can be recorded as a function of temperature and time. Fig. 1 shows the MDSC$^{\mathrm{TM}}$ thermogram of a caesium triborate glass. The solid line represents the total heat flow, where a glass transition at approx. 350°C and a crystallisation at approx. 520°C are displayed. Dashed and dashed-dotted lines represent the reversing and non-reversing components, respectively (see below).

The total heat flow rate is equivalent to the signal recorded by a conventional DSC at the same average heating rate. It is obtained by averaging the raw signal (modulated heat flow rate). The reversing heat flow rate is related to the sample heat capacity, which is given by the ratio between heat flow rate amplitude and heating rate amplitude. Finally, the non-reversing heat flow rate is given by the difference between the total and

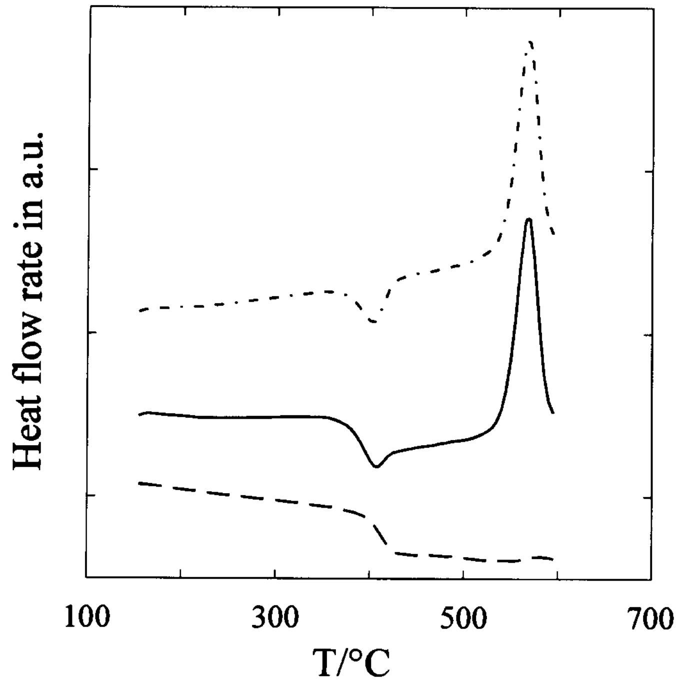

Fig. 1. MDSC curves of a glassy caesium triborate at 10°C/min heating rate. Modulation period is 40 s. Modulation amplitude is 1°C. Solid line, total heat flow rate; dashed-dotted line, non-reversing heat flow rate; dashed line, reversing heat flow rate.

reversing heat flow rates. All signals are deconvoluted from the raw signal by a simple FT process.

It is evident how the choice of modulation period and temperature modulation amplitude could play a fundamental role in the experiment. Since the non-reversing heat flow rate might contain some kinetically-limited components (referred to as $f(T,t)$ in Eq. (3)), the separation between thermodynamic irreversible processes and reversible transitions characterised by a slow kinetics is dependent on the choice of the modulation time-scale. In other words, while the heat flow rate related to true irreversible phenomena (like cold crystallisation) is totally non-reversing and does not depend on period and temperature modulation amplitude (but rather on absolute temperature), a thermodynamic reversible process, e.g. a congruent melting of a crystalline phase, is influenced by the choice of experimental parameters (most notably the heating rate).

3. Experimental

In order to investigate the potential of MDSC™ in materials science, various samples have been prepared and tested, namely: 1. Caesium and rubidium triborate glasses having different thermal histories; 2. A host matrix for ionic electrolytes made with a glass and a polymer; 3. An epoxy–fibre composite material.

3.1. *Caesium and rubidium triborate glasses*

RbB_3O_5 and CsB_3O_5 samples were prepared by fusing a blend of B_2O_3 (Merck, anhydrous pro analysi) and $RbNO_3$ (Aldrich, 99.7%) or $CsNO_3$ (Aldrich, 99%) in a Pt crucible at 1080°C. The melts were kept at this temperature for 30 min after the gas evolution ceased, and finally poured between aluminium blocks at room temperature. Because it is highly hygroscopic, B_2O_3 was previously dehydrated at 800°C until the liquid bubbling ceased, and then quenched down to room temperature; the resulting raw material was immediately used for sample preparation. Both glassy RbB_3O_5 and CsB_3O_5 samples were successively annealed at 320°C (approx. 50°C below T_g) for different amounts of time (from 2 h to 36 d) and ground in an agate mortar just before the measurements were performed. The measured mean particle size was approx. 40 μm.

3.2. *Glass–polymer solid electrolyte*

This sample was prepared by mixing polyethylene oxide (PEO) and sodium triborate glass obtained via sol–gel [10]. Glassy sodium triborate was produced starting from trimethoxyboroxine (Aldrich) and sodium methoxide (Aldrich) as described in Ref. [11]; PEO (BDH Ltd., Polyox wsr-301, molecular weight, 600,000) was dissolved in absolute methanol, stirred for 3 h in a dry box under argon atmosphere, and finally added to the glass before its gelification. The resulting solution was stirred overnight, then cast on a teflon plate at room temperature and kept for 20 h under ambient atmosphere. The sample was dried overnight in a vacuum oven at 60°C.

3.3. *Composite material*

A non-polymerised, pre-impregnated composite material (prepreg), made of an uncured epoxy resin (Cycom 985, Cyanamid) reinforced with carbon fibre, was provided by Agusta S.p.a. (Samarate, Italy). The prepreg, in the form of a film (thickness approx. 0.6 mm), was cured for 2 h at 175°C, and then kept in ambient atmosphere before the measurements.

3.4. *Apparatus*

Measurements were performed on a TA Instruments DSC 10 and a DSC 2920 equipped with modulated DSC^{TM} and a liquid nitrogen cooling accessory (LNCA). The DSC cells were purged with 30 ml/min of dry nitrogen (for glasses) or dry helium (for composites), and calibrated for enthalpy and temperature with both standard indium and zinc. The specific heat capacity calibration was done by means of pure synthetic sapphire.

For all the RbB_3O_5 glassy samples, standard DSC measurements were run at 20°C/min^1, while MDSC^{TM} runs were performed at 10°C/min heating rate. A period of

50 s and a modulation temperature amplitude of ± 1°C were selected. Thermal analyses on composite and glass–polymer materials were also run by MDSC™ at an average underlying heating rate of 10°C/min.

All samples (10 mg to 20 mg) were crimped in standard aluminium DSC pans, in order to insure a good thermal contact between sample and pan.

4. Results and discussion

4.1. Borate glasses

Heat capacity measurements of a number of glassy samples often display some interpretative problems either below the glass transition temperature (T_g) [12, 13] or above it. In fact, in the glassy region some irreversible relaxation phenomena, such as the removal of point defects or (partial) structural rearrangements [14], can take place. However, cold crystallisation may start only a few degrees above the glass transition temperature, thus making it very difficult to measure the metastable liquid heat capacity and its related thermodynamic properties, such as the fictive temperature, T_f, and the difference between glass and metastable liquid heat capacities, ΔC_p [15]. Fig. 2 shows the heat capacities obtained by conventional DSC (solid line), and MDSC (dashed line) of a glassy rubidium triborate annealed for 36 d at a temperature approx. 50°C below T_g. In the C_p curve obtained by conventional DSC, one can notice a sudden heat capacity increase, which describes the glass transition, accompanied by an endothermic peak (T_g overshoot), which is currently related to a structural relaxation

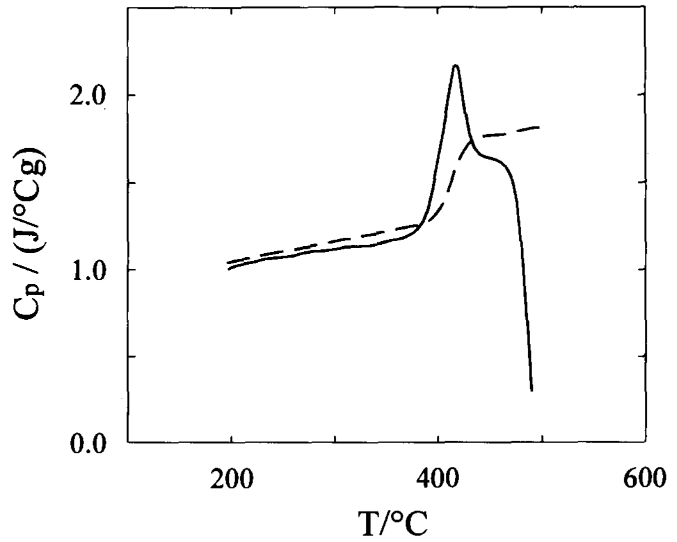

Fig. 2. Heat capacities of a glassy rubidium triborate (annealed 36 d at $T \cong T_g - 50°C$) obtained using conventional DSC (solid line) and MDSC (dashed line).

[16]; the subsequent abrupt fall of the apparent heat capacity is due to cold crystallisation of the metastable liquid phase. This last phenomenon, which is intrinsically irreversible from a thermodynamic point of view, almost completely masks the metastable liquid signal.

In contrast, the MDSC™ heat capacity curve does not show the peak of cold crystallisation. The enthalpy related to the crystallisation process itself does not give any contribution to the heat capacity, which is the sum of two parts: one given by residual glass, and the other by the crystals in formation. In this sense, the heat capacity values may be modified in the temperature range of the crystallisation (see Ref. [17]).

A more detailed comparison between the two graphs leads to two further observations regarding the heat capacity differences in the glassy region near the T_g, and the presence (or absence) of the overshoot peak at the glass transition. The lower heat capacity that conventional DSC sees in a wide temperature range (from approx. 250°C to T_g) is believed to come from irreversible contributions, which are probably related to the removal of structural or point defects frozen in the glass by fast cooling. As a matter of fact, this difference, which is of the order of 7 to 8%, seems too large to be simply caused by errors in the calibration procedure [18]. Of course, this contribution does not affect the heat capacity signal recorded by MDSC™.

The overshoot peak, which only appears in the conventional DSC curve, is believed to depend on the glass relaxation degree [16], and on the heating rate [19]. We recall that overshoot results from a glass structural relaxation and, in particular, that part of the relaxation which takes place in the time of measurement (typically approx. 10^2 s). From this point of view, a suitable choice of the temperature modulation parameters would probably produce an MDSC™ run where this phenomenon is partially seen as reversible, and therefore detectable in the heat capacity curve.

4.2. Glass–polymer solid electrolytes

Our mixed glass–polymer matrix exhibits a complex thermal analysis response; in fact, its DSC thermogram displays a number of thermal effects which may be related to reversible phase changes as well as to irreversible transformations, such as trapped solvent losses or thermal decompositions. Fig. 3 shows an MDSC thermogram of a PEO–sodium triborate sample ($N = [\mathrm{EO}]/[\mathrm{Na}] = 1$) from room temperature up to 200°C. In the total heat curve (solid line), three distinct endotherms (A, B, C) are detected. The deep peak at approx. 50°C (A) is also present in the reversing curve (dotted line), and can be easily associated with melting of the PEO crystalline phase [20]. The two other endotherms (B and C), in contrast, are well represented in the non-reversing heat flow (dashed line): this seems to suggest a true irreversible phenomenon (at least in the limits of the experimental conditions, see below), which may be associated with losses of water present in the sample, as suggested by preliminary TG-FTIR runs.

We recall that a proper choice of the modulation parameters is crucial: whenever the number of wave cycles inside the peak is not enough to enable the deconvolution algorithm to operate properly, the separation of the signals will be in error. This may

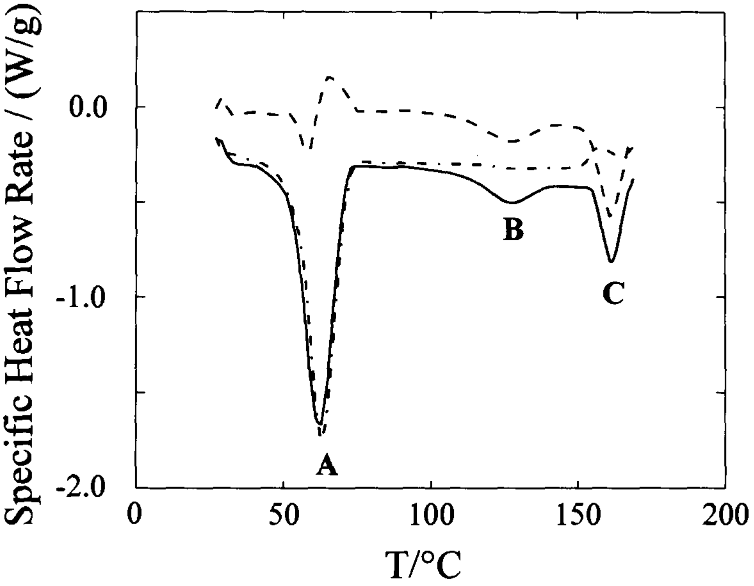

Fig. 3. MDSC curves of a (1:1) PEO/Na_2O:$3B_2O_3$ matrix at 10°C/min. Modulation period is 40 s. Modulation amplitude is 1°C. Solid line, total heat flow rate; dashed-dotted line, non-reversing heat flow rate; dashed line, reversing heat flow rate.

clearly be seen in the region of peak A, where the non-reversing curve displays an artefact. For the same reason, the reversing curve is affected by a large artefact in the region of the narrow peak C, whereas it happens to a lower extent for peak B, whose width at half height (approx. 20°C) is large enough to allow the completion of about three modulation cycles. However, a good rule of thumb is to allow at least five full cycles to run through the peak width at half height. For more details, see Ref. [8].

4.3. Composites

Fig. 4 represents an MDSC^{TM} thermogram of the epoxy–carbon polymerised sample. The total heat flow rate, corresponding to the heat flow rate obtained by a conventional DSC, is rather complex in the glass transition region because of some residual curing, and does not allow a precise estimation of the T_g. It is quite evident, in fact, that a determination of T_g performed on the basis of a conventional DSC curve (equivalent to the total heat flow rate of Fig. 4) could lead to an error of more than 50°C. The MDSC^{TM} reversing signal, in contrast, displays a neat baseline, where the change corresponding to the T_g is easily detectable. Finally, the shape of the "non-reversing" signal is substantially determined by the residual curing, which is a true irreversible process.

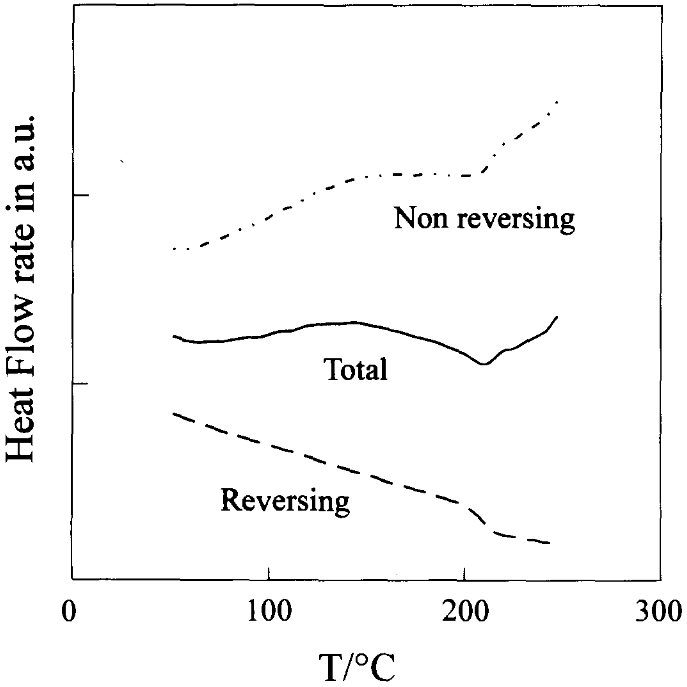

Fig. 4. MDSC curves of composite material (see text) at 5°C/min. Modulation period is 50 s. The modulation amplitude is 0.66°C. Solid line, total heat flow; dashed-dotted line, reversing heat flow dashed line, non-reversing heat flow.

5. Conclusions

We have shown that modulated DSC™ may be very useful in thermal characterisation of amorphous and partially crystalline materials. Amongst its capabilities, we see the possibility of separating contributions to the heat capacity that are not fully thermodynamically reversible. Another important result is the discrimination between reversing and non-reversing phenomena, at least in terms of the chosen experimental parameters.

We stress, however, that this last point is very crucial, since artefacts may be generated if there are insufficient modulation cycles over the temperature range of the transition. Reducing the underlying average heating rate will mostly eliminate this problem.

References

[1] C.S. Ray, W. Huang and D.E. Day, J. Am. Ceram. Soc., 74 (1991) 60.
[2] G.S. Grest and M.H. Cohen, Phys. Rev. B, 21 (1980) 4113.
[3] K.F. Kelton, J. Non-Cryst. Solids, 163 (1993) 283.

[4] R.F. Speyer and S.H. Risbud, Adv. Ceram., 4 (1982) 182.
[5] N.P. Bansal, A.J. Bruce, R.H. Doremus and C.T. Moynihan, Phys. Chem. Glasses, 25 (1984) 86.
[6] R.F. Speyer and S.H. Risbud, Phys. Chem. Glasses, 25 (1984) 86.
[7] R. Ciach, W. Kapturkiewicz, W. Wolczynsky and A.M. Zahra, J. Therm. Anal., 38 (1992) 1949.
[8] P.S. Gill, S.R. Sauerbrunn and M. Reading, J. Therm. Anal., 40 (1993) 931.
[9] A. Marini, in A. Bellosi (Ed.), Caratterizzazione e reattività di materiali speciali, CNR-IRTEC, Faenza, 1989, p.1 (in Italian).
[10] A. Magistris, P. Ferloni, P. Mustarelli, M. Restelli and G. Chiodelli, New mixed glass-polymer solid electrolytes, in B.V.R. Chowdari, M. Yahaya, I.B. Talib and M.M. Salleh (Eds.), Solid State Ionic Materials, World Scientific, Singapore, 1994, p.361.
[11] N. Venkatasubramanian, B. Wade, P. Desai, A.S. Abhiraman and L.T. Gelbaum, J. Non-Cryst. Solids, 130 (1991) 144.
[12] L. Avramov and I. Gutzow, J. Non-Cryst. Solids, 104 (1988) 148.
[13] S.N. Crichton and C.T. Moynihan, J. Non-Cryst. Solids, 99 (1988) 413.
[14] C.A. Angell, J. Non-Cryst. Solids, 102 (1988) 205.
[15] C.T. Moynihan, A.J. Easteal, M.A. DeBolt and J. Tucker, J. Am. Ceram. Soc., 59 (1976) 12.
[16] L. Boehm, M.D. Ingram and C.A. Angell, J. Non-Cryst. Solids, 44 (1981) 305.
[17] M. Reading, A. Luget and R. Wilson, Thermochim. Acta, 238 (1994) 295.
[18] B. Wunderlich, Y.M. Jin and A. Boller, Thermochim. Acta, 238 (1994) 277.
[19] M.A. DeBolt, A.J. Easteal, P.B. Macedo and C.T. Moynihan, J. Am. Ceram. Soc., 59 (1976)16.
[20] P. Ferloni, G. Chiodelli, A. Magistris and M. Sanesi, Solid State Ionics, 18–19 (1986) 265.